

In(Ga)As/GaAs Quantum Dots for Optoelectronic Devices

K. Sears*, S. Mokkapati, M. Buda, H. H. Tan, C. Jagadish

Department of Electronic Materials Engineering, Research School of Physical Sciences and Engineering, The Australian National University, Canberra, ACT, 0200, Australia

ABSTRACT

This paper discusses the self-assembled growth of In(Ga)As/GaAs quantum dots by metal-organic chemical vapor deposition and their application to diode lasers and integrated opto-electronic devices. After an extensive study of the growth parameters high densities ($3-4 \times 10^{10} \text{cm}^{-2}$) of defect free quantum dots have been achieved and ground state lasing demonstrated for diode lasers with 5 stacked layers of quantum dots in the active region. This presentation will review the important growth parameters and the lasing characteristics of quantum dot lasers. Results for selective area epitaxy of quantum dots using SiO_2 patterning will also be presented. Selective area epitaxy has been used to form quantum dots with different wavelength/bandgap in different regions of a GaAs substrate and has led to the integration of a quantum dot laser and waveguide.

Keywords: quantum dots, QD diode lasers, selective area epitaxy, MOCVD, In(Ga)As, photonic integrated circuits

1. INTRODUCTION

Quantum dot devices are predicted to have superior performance in comparison to their quantum well (QW) counterparts due to their 3 dimensional carrier confinement and discrete delta-like density of states. Among the advantages predicted for quantum dot lasers are lower threshold currents, improved efficiencies and greater thermal stability [1,2]. With the discovery that semiconductor quantum dots could be formed in the Stransk-Krastanow growth mode, quantum dot lasers have become a reality and many of their predicted advantages have been demonstrated. For example low threshold currents on the order of 20 A/cm^2 per dot layer [3-5] and high thermal stability with characteristic temperatures as high as 300 K at room temperature [5-7] have been reported. Lasing at 1.3 and $1.5 \mu\text{m}$ for telecommunications has also been achieved by capping InAs quantum dots with thin InGaAs capping layers [4,8,9].

However it is still difficult to achieve all of the above characteristics in the one device, with only a few such reports [5,6]. Furthermore, most studies to date use molecular beam epitaxy (MBE) as the growth technique, while there are few reports of InAs/GaAs quantum dots and quantum dot diode lasers grown using metal-organic chemical vapor deposition (MOCVD), despite its importance in industry. After an extensive study of the growth parameters we have achieved single and stacked layers of In(Ga)As quantum dots using MOCVD and have successfully demonstrated QD diode lasers. This paper will give an overview of the important quantum dot growth parameters and the lasing characteristics of diode lasers with 5 stacked layers of In(Ga)As quantum dots in the active region.

The monolithic integration of QD devices, such as a waveguide with a QD laser, is also desirable because it enables low loss, high speed modules, operating at lower currents. To this end we have used the technique of selective area epitaxy (SAE) to form quantum dots emitting at different wavelengths in different parts of the same wafer through patterning with a SiO_2 mask. This work will be described and has led to the demonstration of multi-wavelength diode lasers on the same wafer as well as the integration of a quantum dot laser with a waveguide.

2. EXPERIMENTAL DETAILS

All of the results presented in this paper are for samples grown on (001) GaAs substrates using a low-pressure (100mbar) AIXTRON 200/4, horizontal flow MOCVD reactor. The sources used were trimethylindium, trimethylgallium and AsH_3 , with H_2 as the carrier gas. For the laser structures silane and CCl_4 were used for n and p type doping, respectively. Fig. 1 shows a schematic of the standard structure used to optimize the quantum dot growth. It consists of a layer of

buried quantum dots for both photoluminescence (PL) measurements and transmission electron microscopy (TEM) studies. After capping the buried quantum dots with a 300nm layer of GaAs, a final layer of dots was deposited on the surface and left uncapped for atomic force microscopy (AFM).

PL measurements were performed at either 77K or room temperature by exciting the samples with a frequency-doubled 532nm diode-pumped solid state laser source. The luminescence was dispersed through a 0.5m monochromator and collected with an InGaAs detector. Samples for plan-view TEM were prepared by mechanically polishing the samples to 150 μ m, followed by dimpling to a thickness of 40 μ m and chemically etching with H₂SO₄:H₂O₂:H₂O (3:1:1) to electron transparency. TEM analysis was carried out using a Philips CM300 electron microscope instrument operated at 200kV. For the selective area epitaxy samples cathode-luminescence measurements were also made. An Oxford Instruments MonoCL2 system installed on a Jeol 35C scanning electron microscope was used and the samples excited using a 13 kV electron beam.

Thin p-clad laser structures with stacked layers of QDs in the active region were fabricated as shown in Fig. 2. The quantum dot active region is sandwiched between two 0.16 μ m undoped AlGaAs graded index layers. In order to minimize the time spent by the QDs at elevated temperatures the top p-cladding layer is kept thin and consists of a 0.45 μ m Al_{0.45}Ga_{0.55}As confinement layer and a 0.1 μ m highly doped GaAs contact layer. This is important because the quantum dots are highly sensitive to the growth temperature used for the overlayers [10]. The n-cladding layer is much thicker and consists of a 1.8 μ m Al_{0.45}Ga_{0.55}As and 0.25 μ m Al_{0.3}Ga_{0.7}As layer. Further details on the laser can be found in references [11,12].

The structures were fabricated into 4 μ m ridge waveguides using standard lithography and wet chemical etching. The mirror facets were left as cleaved (no reflectivity coatings applied) and the devices tested at 7 and 20°C in pulsed mode with a duty cycle of 5% (25kHz, 2 μ s pulse). The quoted threshold current density values are based on the ridge waveguide area. A comparison of 4 and 50 μ m ridge waveguide lasers indicates that current spreading effects exaggerated the threshold current density values of the 4 μ m ridge waveguide lasers by a factor of 2-2.5.

For the SAE work, the SiO₂ was deposited at 300°C by plasma enhanced chemical vapor deposition and patterned using standard photolithography and etching in a buffered HF solution. Further details can be found in reference [13].

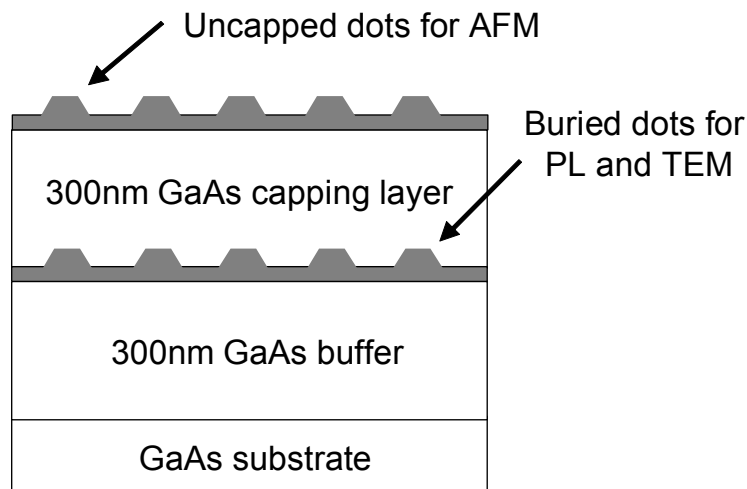


Fig 1. Schematic of the sample structure grown to optimize the QD growth parameters.

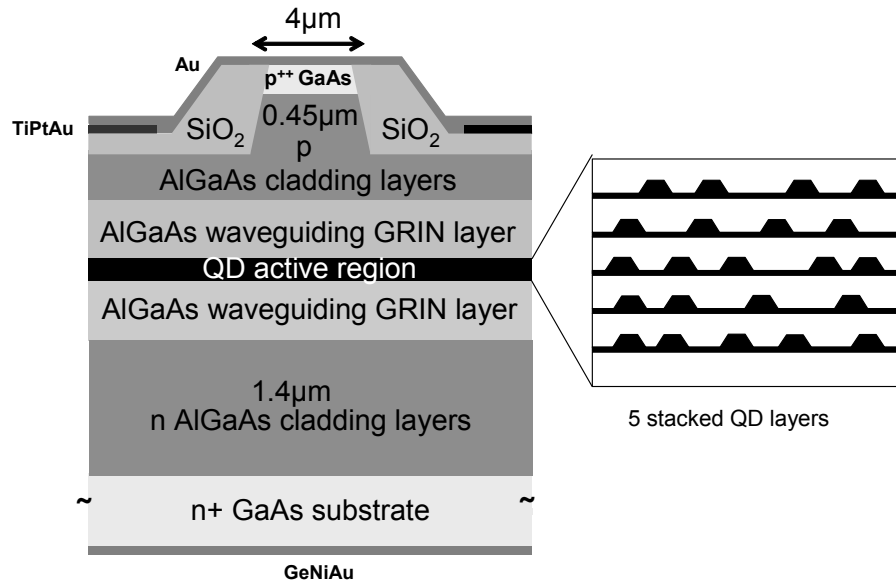


Fig. 2. Schematic of the thin p-clad laser structure

3. SELF-ASSEMBLED GROWTH OF IN(GA)AS QUANTUM DOTS

Quantum dot formation in the Stranski-Krastanow (S-K) growth mode relies on a slight lattice mismatch between the epilayer and substrate. This mismatch is $\sim 7.2\%$ for InAs on GaAs and $\sim 3.1\%$ for $\text{In}_{0.5}\text{Ga}_{0.5}\text{As}$ on GaAs, the two compositions considered in this paper. In the S-K mode, growth initially proceeds in a layer by layer fashion and the strain is accommodated through biaxial compression of each layer. However with increasing layer thickness the strain energy accumulates until at some critical thickness it becomes energetically favorable for island formation. This critical thickness is ~ 4.5 monolayers (ML) for $\text{In}_{0.5}\text{Ga}_{0.5}\text{As}$ on GaAs and 1.7ML for InAs on GaAs. While the driving force for island formation is clearly a thermodynamic one, the growth parameters used have a strong influence over the characteristics of the final island ensemble. This is particularly the case for InAs/GaAs QDs where their high strain makes them very sensitive to almost all of the growth parameters. The important MOCVD growth parameters and their influence on QD formation are discussed in the following sections.

3.1 Amount of material deposited (coverage)

The amount of material deposited, or coverage, is one of the most important growth parameters. Fig. 3 shows 77K photoluminescence spectra and AFM images for $\text{In}_{0.5}\text{Ga}_{0.5}\text{As}$ quantum dot samples grown using different coverages. This illustrates nicely the S-K growth mode. At the lowest coverage of 3.3ML, the critical thickness has not yet been exceeded so that only a thin quantum well (known as the wetting layer) is formed. PL from this thin wetting layer is observed at $\sim 890\text{nm}$ with a relatively narrow linewidth. As more material is deposited the dot density and size increases. The QD PL correspondingly grows in intensity and shifts to longer wavelength. In this example the QD density saturates at 5.7ML. Deposition of further material leads to an increased island size until eventually large clustered islands form. These islands tend to relax via defect formation and grow at the expense of the surrounding islands resulting in an overall reduction in island density and size. This results in the lower PL intensity observed for the 8.3ML sample.

The effect of coverage on InAs/GaAs QD formation is similar except that the higher strain of this system results in a much faster nucleation process. As a consequence, a high density of defect free InAs quantum dots can only be formed over a narrow range of coverages [14].

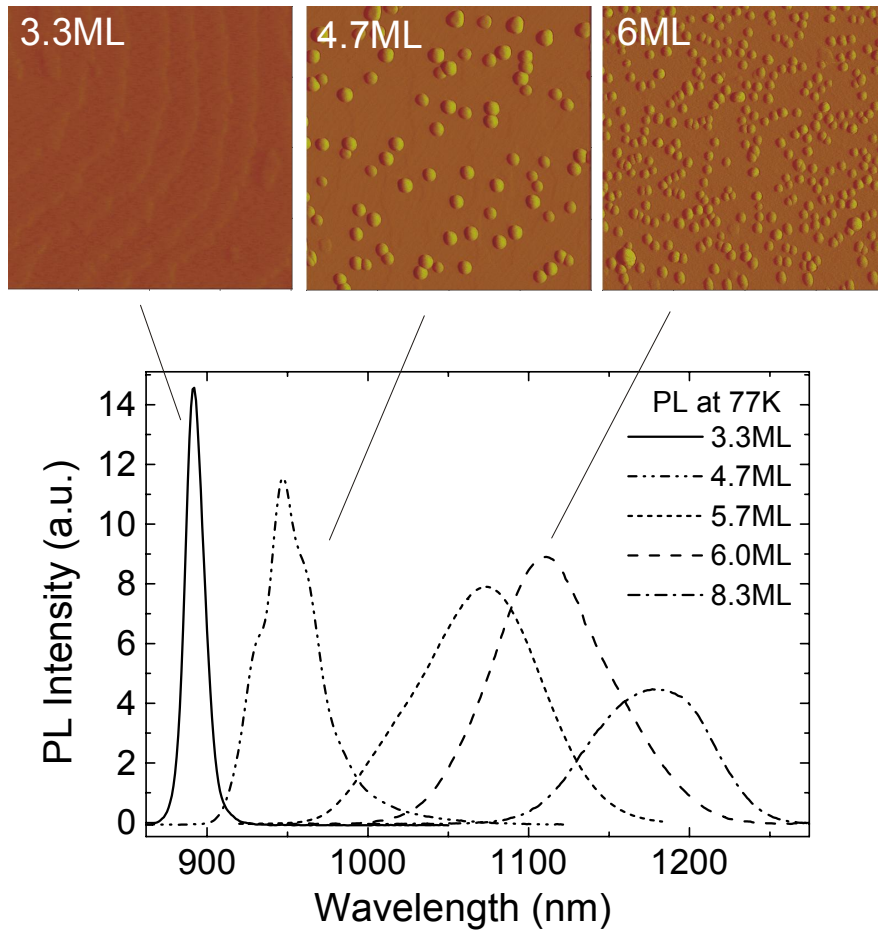


Fig. 3. 77K photoluminescence spectra and $1 \times 1 \mu\text{m}^2$ deflection AFM images for $\text{In}_{0.5}\text{Ga}_{0.5}\text{As}$ quantum dot samples formed using different coverages. The dots were deposited at their optimum growth temperature of 550°C with a growth rate of 1.7ML/s .

3.2 QD Growth Temperature

Temperature affects the adatom mobility and therefore has a large influence on the nucleation process. In order to reduce the adatom mobility and tendency for island coalescence it is important to grow quantum dots at growth temperatures between $450\text{--}550^\circ\text{C}$ [15,16]. However these temperatures are much lower than those conventionally used in MOCVD and can lead to grown in defects due to incomplete cracking of the precursor gases. Despite this, high quality InAs and $\text{In}_{0.5}\text{Ga}_{0.5}\text{As}$ quantum dots were formed for optimum growth temperatures of 520 and 550°C , respectively.

The affect of growth temperature on QD formation is illustrated by Fig. 4, which shows room temperature PL spectra for InAs QDs grown at different temperatures. With increasing growth temperature the PL shifts to longer wavelength which is characteristic of larger QDs and in agreement with an increased diffusion length. An improved cracking efficiency may also contribute to this red-shift through both an increased deposition rate and a possible change in the V/III ratio. The strong room temperature PL intensity indicates that the quantum dots are of good quality. At the highest growth temperature the PL intensity drops. This is likely due to the increased tendency for larger islands to plastically relax via defect formation, particularly in the case of InAs/GaAs QDs where the strain is high. To determine the optimum growth temperature, a study of coverage was made at each growth temperature.

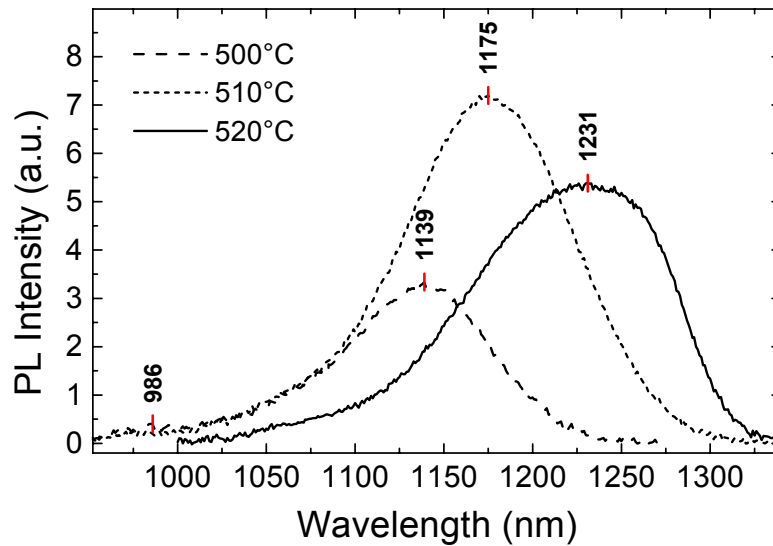


Fig. 4. Room temperature photoluminescence spectra of InAs quantum dot samples grown at different temperatures. The dots were formed using a nominal deposition rate and coverage of 0.5ML/s and 1.65ML respectively.

3.3 AsH₃ flow (or V/III ratio)

The V/III ratio is the ratio of the Group V precursor gases (AsH₃) to the group III precursor gases (TMGa and TMIIn). The AsH₃ flow, both during growth and afterwards during a growth interrupt, has a large effect on island formation [14,17]. High AsH₃ flows were found to encourage island ripening with the formation of large plastically relaxed islands. Therefore low AsH₃ flows during growth, in our case corresponding to V/III ratios between 10 and 40, are critical to obtain defect free quantum dot ensembles.

Another method of forming islands is to deposit just enough material so that island formation occurs during a subsequent growth interrupt. A growth interrupt involves interrupting the growth for a short period of time during which the precursor gases are switched off. Due to the high strain in the In(Ga)As/GaAs system, material continues to redistribute even after the precursors are switched off [14,18,19]. In order to achieve defect free InAs/GaAs quantum dots we have found it critical to switch off the AsH₃ flow during growth interruption[14]. This is contrary to standard MOCVD practice where it is usual to maintain an AsH₃ flow at all times, in order to avoid outdiffusion of As from the sample surface.

4. GROWTH OF STACKED QUANTUM DOT LAYERS

Stacked QD layers are needed to ensure sufficient ground state gain for lasing. QDs formed in the Stranski-Krastanow growth mode typically have densities between 10^9 and 10^{11} cm⁻². The optimized growth conditions for our InAs and In_{0.5}Ga_{0.5}As QDs result in QD densities of 3 and 4×10^{10} cm⁻², respectively. These densities correspond to a low surface coverage, 10-20% that of a quantum well. Furthermore, because of the large QD size distribution, only a subset of the islands contribute to the gain at any particular wavelength. Consequently, the gain provided by a single layer of QDs is typically insufficient for ground state lasing and stacks of three to five QD layers are needed [9,20].

In order to successfully stack dot layers it is important to replanarize the growth front of the GaAs spacer layer before depositing the next layer of quantum dots. The surface morphology of the spacer layer is extremely important because it affects both island nucleation and the optical scattering losses of a device. Fig. 5 shows AFM images of the top In_{0.5}Ga_{0.5}As quantum dot layer of a 3 stacked structure grown with and without surface smoothing techniques. Each dot layer is separated by a 30nm spacer layer which is sufficiently thick to avoid vertical coupling of the quantum dots [21-23]. With no surface smoothing the top dot layer has a density half that of a single layer. However with surface smoothing techniques, the dot density in the top layer is nearly identical to that of a single layer.

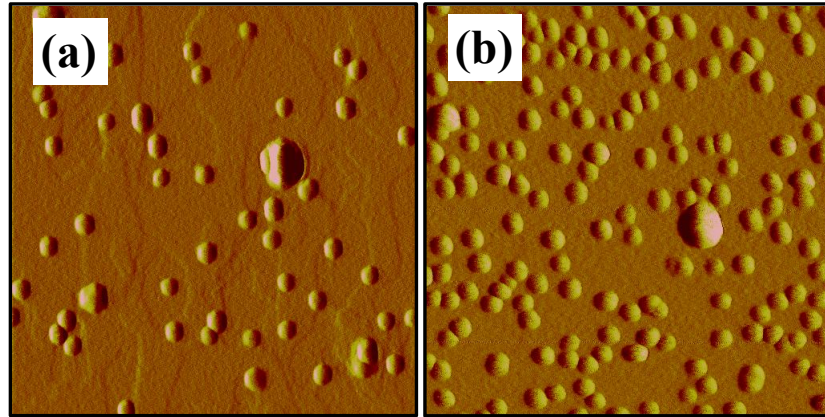


Fig. 5. $500 \times 500 \text{ nm}^2$ AFM deflection images of the top $\text{In}_{0.5}\text{Ga}_{0.5}\text{As}$ dot layer in a 3 stacked structure (a) with no surface smoothing and (b) with surface smoothing.

The surface smoothing techniques rely on increasing the adatom mobility. In the case of $\text{In}_{0.5}\text{Ga}_{0.5}\text{As}$ quantum dots, the introduction of a 1.5 minute growth interrupt after capping the dots with 7nm of GaAs is sufficient to replanarise the surface. In the case of InAs/GaAs quantum dots, the strain is much greater and influences the GaAs overgrowth strongly. Therefore the smoothing procedure relies on (i) increasing the growth temperature from 520°C (that of the quantum dots) to 600°C and (ii) reducing the GaAs depositing rate from 6 to 3 \AA/s , for the final 20nm of the GaAs spacer layer.

5. QD LASERS

The optimized InAs/GaAs and $\text{In}_{0.5}\text{Ga}_{0.5}\text{As}$ /GaAs quantum dot lasers showed similar lasing characteristics. In each case, 5 layers of QDs were needed to achieve ground state lasing. Fig. 6 shows a lasing spectrum from a 5 stacked InAs/GaAs quantum dot laser with a cavity length of 4.5 mm. Also shown for comparison is a PL spectrum of the same sample prior to device fabrication. The lasing spectrum coincides with the PL peak indicating that the device lases predominantly from the QD ground state. Also shown in the inset is a plot of inverse differential efficiency versus device length. A linear fit to this data gives an optical loss of $\sim 8 \text{ cm}^{-1}$ and an internal efficiency close to 100%.

Fig. 7 shows plots of lasing wavelength and threshold current density as a function of device length for the same InAs/GaAs 5-stack QD lasers. The 5-stack QD lasers continue to operate from the QD ground state for device lengths as short as 1.5mm. As the cavity length is decreased beyond this length, the emission wavelength decreases rapidly while the threshold current density increases. Clearly the ground state gain is insufficient to overcome the higher losses of these short devices. Consequently the excited and wetting layer states, which are capable of providing greater gain [24,25], are populated resulting in shorter output wavelengths and increased threshold currents. Work has also indicated that population of the excited and wetting layer states can lead to increased non-radiative recombination [26].

6. SELECTIVE AREA EPITAXY

Selective area epitaxy (SAE) has been used to spatially control the nucleation of quantum dots on a GaAs substrate in a single growth. In SAE, the substrate is patterned with a mask of dielectric material, in our case SiO_2 . A schematic of the typical mask used in our work is shown on the left side of Fig. 8. It consists of pairs of SiO_2 stripes of varying dimensions. In the example shown, the opening between the stripes is kept constant at $50 \mu\text{m}$, while the width of the SiO_2 stripes is varied. Epitaxial growth does not take place on the SiO_2 mask. Instead, material deposited on the SiO_2 migrates toward the mask openings, enhancing the growth rate there. The wider the SiO_2 stripes or narrower the mask openings, the greater the growth enhancement in the mask openings. The quantum dot nucleation can therefore be spatially controlled by changing the local mask dimensions.

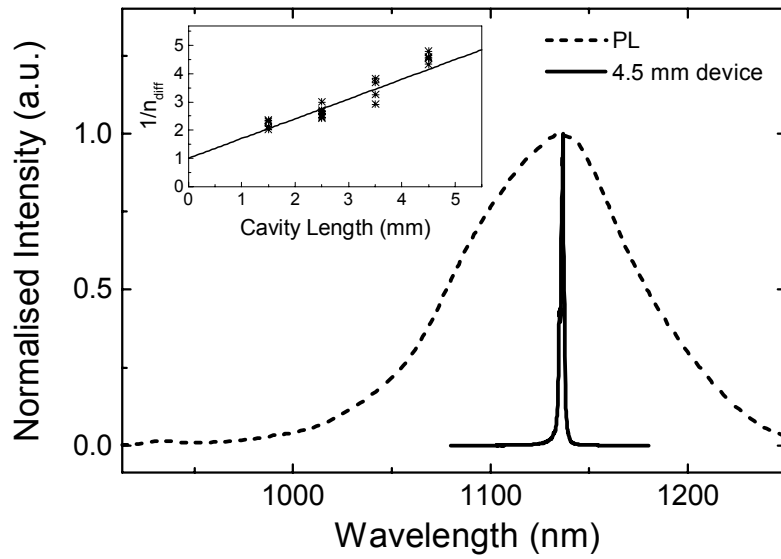


Fig. 6. Photoluminescence and lasing spectra for a 5 stack InAs/GaAs quantum dot diode laser. The PL spectrum was measured prior to device fabrication. The inset shows a plot of inverse differential efficiency versus cavity length.

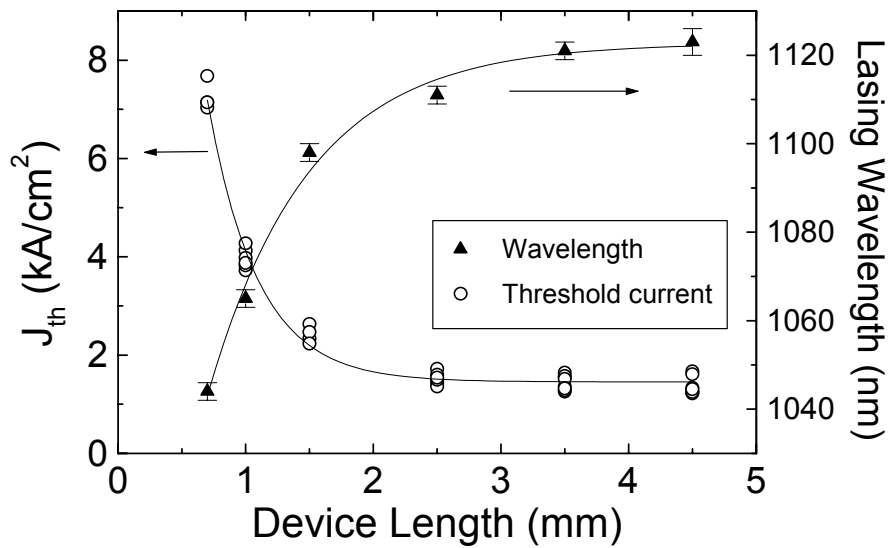


Fig. 7. Threshold current density and lasing wavelength versus device length for a 5 stack InAs QD laser. The line fits are shown as a guide only.

Fig. 8 shows plan-view TEM images and CL spectra for InAs deposited on a wafer patterned with an SAE mask as shown. In this example $\sim 1.2\text{ML}$ of InAs was deposited (in the unpatterned region) which is just below the critical thickness for InAs island formation. For the smallest stripe width of $15\mu\text{m}$, the growth enhancement is insufficient for the 2D-3D critical thickness to be exceeded. Therefore no islands form and only CL from the thin wetting layer is observed at 1020nm . At a stripe width of $25\mu\text{m}$ the growth enhancement is sufficient for the formation of a high density of quantum dots. This is reflected in the CL spectrum where strong QD emission is observed at 1090nm . As the stripe width is further increased, the island size and density increases leading to a redshift of the quantum dot CL. However the plan-view TEM image also shows that defects have formed (see arrow in fig. 8 (a)). This is typical for InAs QDs, where larger islands are very susceptible to defect formation[10,14].

These results clearly show that quantum dots with different bandgaps can be selectively grown in different regions of the same substrate in a single growth. Similar studies have been performed with $\text{In}_{0.5}\text{Ga}_{0.5}\text{As}$ quantum dots in which quantum dots with luminescence at wavelengths between 1150 and 1230 nm could be achieved in different parts of the same wafer [13]. This process has been used to fabricate $\text{In}_{0.5}\text{Ga}_{0.5}\text{As}$ quantum dot lasers emitting at different output wavelengths on a single substrate. Fig. 9 shows electroluminescence spectra for two such lasers. A stripe opening of $50\mu\text{m}$ was used in each case, while stripe widths of either 5 or $15\mu\text{m}$ were used.

SAE has also been used to integrate an $\text{In}_{0.5}\text{Ga}_{0.5}\text{As}$ quantum dot laser with a low loss passive waveguide [27]. In order to achieve low loss waveguides, it is essential that the bandgap of the waveguide material is greater than that of the quantum dots so that the waveguide is transparent to the laser light. This has been achieved by choosing appropriate mask dimensions so that the 2D-3D critical thickness is only exceeded in the laser region while in the waveguide region only a thin quantum well (or wetting layer) forms. This enables a large bandgap difference of 200meV between the laser and waveguide material and low waveguide losses of $\sim 3\text{ cm}^{-1}$ [27].

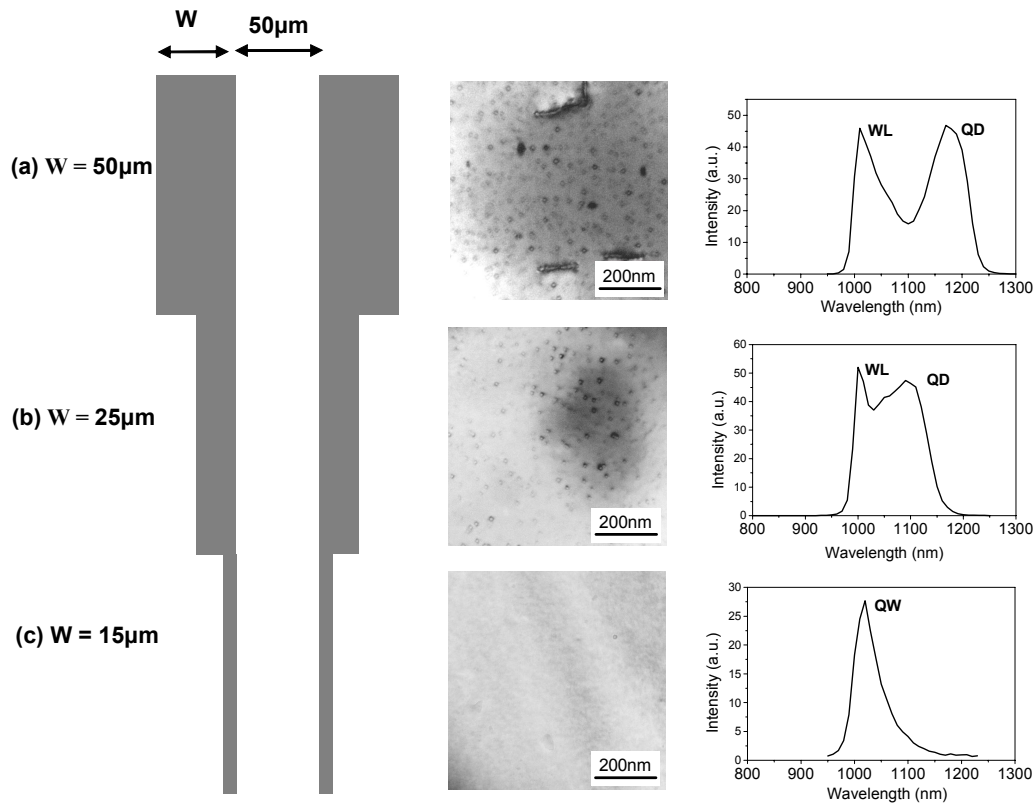


Fig. 8. Schematic of the SAE mask used showing three regions with different SiO₂ stripe widths. CL spectra and plan view TEM images are shown next to each mask region and illustrate how the mask dimensions can be varied to spatially control island nucleation. The CL measurements were made at 77K

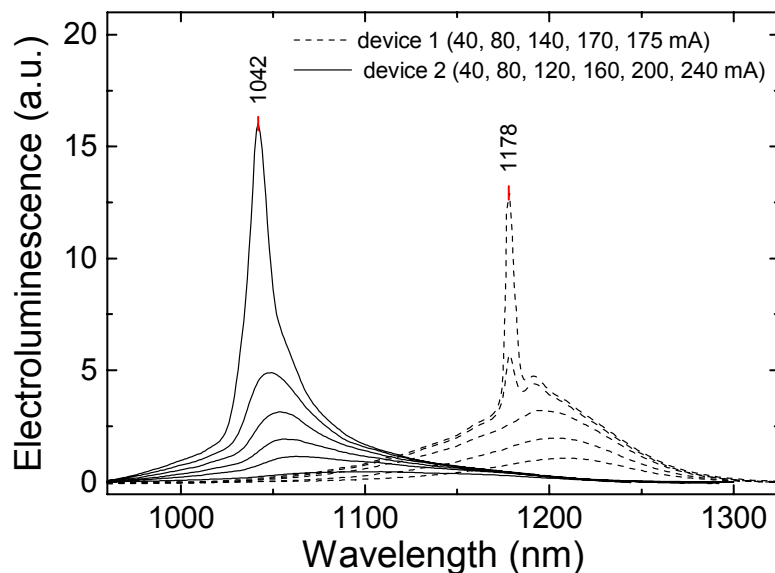


Fig. 1. Electroluminescence spectra measured at various injection currents up to the lasing threshold for two $\text{In}_{0.5}\text{Ga}_{0.5}\text{As}$ quantum dot devices. The two lasers were fabricated from different regions of the same wafer patterned with an SAE mask. The opening between the SAE stripes was $50\mu\text{m}$ in each case while the stripe width was either $5\mu\text{m}$ (device 2-solid curves) or $15\mu\text{m}$ (device 1-dashed curves).

7. CONCLUSION

The important growth parameters for $\text{In}(\text{Ga})\text{As}/\text{GaAs}$ quantum dot formation have been discussed. Using our optimized growth conditions single and stacked layers of defect free dots with a density of $\sim 3\text{-}4 \times 10^{10} \text{cm}^{-2}$ have been grown. Ground state lasing and good device performance has been achieved for diodes lasers with 5 stacked layers of $\text{In}(\text{Ga})\text{As}$ quantum dots in the active region. Finally selective area epitaxy has been used to spatially control quantum dot nucleation on a GaAs substrate in a single growth. The ability to form areas with and without QDs on the same substrate has led to the integration of a low loss waveguide ($\sim 3 \text{cm}^{-1}$) with a QD laser.

8. ACKNOWLEDGMENTS

Thanks are due to Dr. Manuela Buda and Mr. Michael Aggett for fruitful discussions and expert technical advice, respectively. We also wish to acknowledge Dr Vince Craig, and John FitzGerald for their expert advice on AFM and TEM respectively. The Australian Research Council is gratefully acknowledged for their financial support.

REFERENCES

1. R. Dingle and C. H. Henry, "Quantum effects in heterostructure lasers," *U.S. Patent* (3982207), (1976).
2. Y. Arakawa and H. Sakaki, "Multidimensional quantum well laser and temperature dependence of its threshold current," *Appl. Phys. Lett.* 40(11): 939 (1982).
3. G. T. Liu, H. Li. Stintz, T. C. Newell, A. L. Gray, P. M. Varangis, K. J. Malloy and L. F. Lester, "The influence of quantum-well composition on the performance of quantum dot lasers using InAs/InGaAs dots-in-a-well (DWELL) structures," *IEEE J. Quantum Electron.* 36(11): 1272 (2000).
4. I. R. Sellers, H. Y. Liu, K. M. Groom, D. T. Childs, D. Robbins, T. J. Badcock, M. Hopkinson, D. J. Mowbray and M. S. Skolnick, "1.3 μm InAs/GaAs multilayer quantum-dot laser with extremely low room-temperature threshold current density," *Electron. Lett.* 40(22): 1412 (2004).
5. A. R. Kovsh, N. A. Maleev, A. E. Zhukov, S. S. Mikhlin, A. P. Vasil'ev, Yu. M. Shernyakov, M. V. Maximov, D. A. Livshits, V. M. Ustinov, Zh. I. Alferov, N. N. Ledentsov and D. Bimberg, "InAs/InGaAs/GaAs quantum dot lasers of 1.3 μm range with high (88%) differential efficiency," *Electron. Lett.* 38(19):1104 (2002).
6. O. B. Shchekin and D. G. Deppe, "1.3 μm quantum dot laser with $T_0=161\text{K}$ from 0 to 80°C," *Appl. Phys. Lett.* 80(18): 3277 (2002).
7. M. V. Maximov, I. V. Kochnev, Y. M. Shernyakov, S. V. Zaitsev, N. Yu. Gordeev, A. F. Tsatsul'nikov, A. V. Sakharov, I. L. Krestnikov, P. S. Kop'ev, Zh. I. Alferov, N. N. Ledentsov, D. Bimberg, A. O. Kosogov, P. Werner and U. Gösele, "InGaAs/GaAs quantum dot lasers with ultrahigh characteristic temperature ($T_0=385\text{K}$) grown by metal organic chemical vapour deposition," *Jpn J. Appl. Phys.* 36(6B): 4221 (1997).
8. N. N. Ledentsov, A. R. Kovsh, A. E. Zhukov, N. A. Maleev, S. S. Mikhlin, A. P. Vasil'ev, E. S. Semenova, M. V. Maximov, Yu. M. Shernyakov, N. V. Kryzhanovskaya, V. M. Ustinov and D. Bimberg, "High performance quantum dot lasers on GaAs substrates operating in 1.5 μm range," *IEEE Photon. Technol. Lett.* 39(15): 1126 (2003).
9. A. E. Zhukov, A. R. Kovsh, V. M. Ustinov, Yu. M. Shernyakov, S. S. Mikhlin, N. A. Maleev, E. Yu. Kondrat'eva, D. A. Livshits, M. V. Maximov, B. V. Volovik, D. A. Bedarev, Yu. G. Musikhin, N. N. Ledentsov, P. S. Kop'ev, Zh. I. Alferov and D. Bimberg, "Continuous-wave operation of long-wavelength quantum-dot diode laser on a GaAs substrate," *IEEE Photon. Technol. Lett.* 11(11): 1345 (1999).
10. K. Sears, J. Wong-Leung, M. Buda, H. H. Tan and C. Jagadish, "Growth and characterization of InAs/GaAs quantum dots grown by MOCVD," *Proceedings of the 2004 Conference on Optoelectronic and Microelectronic Materials and Devices*, Brisbane, Australia, pp. 1-4 (2004)
11. M. Buda, J. Hay, H. H. Tan, J. Wong-Leung and C. Jagadish, "Low loss, thin p-clad 980-nm InGaAs semiconductor laser diodes with an asymmetric structure design," *IEEE J. Quantum Electron.* 39(5): 625 (2003).
12. M. Buda, J. Hay, H. H. Tan and C. Jagadish, "Thin clad diode laser," *US patent* (6): 993, 053 (2006).
13. S. Mokkapatil, P. Lever, H. H. Tan, C. Jagadish, K. E. McBean and M. R. Phillips, "Controlling the properties of InGaAs quantum dots by selective-area epitaxy," *Appl. Phys. Lett.*, 86, 113102:1-3 (2005).
14. K. Sears, H. H. Tan, J. Wong-Leung and C. Jagadish, "The role of arsine in the self-assembled growth of InAs/GaAs quantum dots by metal organic chemical vapor deposition," *J. Appl. Phys.*, 99, 044908:1-5 (2006)
15. A. A. El-Emawy, S. Birudavolu, P. S. Wong, Y.-B. Jiang, H. Xu, S. Huang, D. Huffaker, "Formation trends in quantum dot growth using metalorganic chemical vapor deposition," *J. Appl. Phys.* 66, 081305 (2003) .
16. J. Tatebayashi, M. Nishioka, Y. Arakawa, "Over 1.5 μm light emission from InAs quantum dots embedded in InGaAs strain-reducing layer grown by metalorganic chemical vapor deposition," *Appl. Phys. Lett.* 78, 3469 (2001).
17. T. Chung, G. Walter and N. Holonyak Jr., "Growth mechanism of InAs quantum dots on GaAs by metal-organic chemical-vapor deposition," *J. Appl. Phys.*, 97: 53 510 (2005).
18. K. Pötschke, L. Müller-Kirsch, R. Heitz, R. L. Sellin, U. W. Pohl, D. Bimberg, N. Zakharov and P. Werner, "Ripening of self-organized InAs quantum dots," *Physica E*, 21: 606 (2004).
19. H. Lee, R. Lowe-Webb, W. Yang and P. Sercel, "Formation of InAs/GaAs quantum dots by molecular beam epitaxy: Reversibility of the islanding transition," *Appl. Phys. Lett.* 71(16): 2325 (1997).
20. O. G. Schmidt, N. Kirstaedter, N. N. Ledentsov, M.-H. Mao, D. Bimberg, V. M. Maximov, P. S. Kop'ev and Zh. I. Alferov, "Prevention of gain saturation by multi-layer quantum dot lasers," *Electron. Lett.* 32(14): 1302 (1996).
21. Q. Xie, A. Madhukar, P. Chen and N. P. Kobayashi, "Vertically self-organized InAs quantum box islands on GaAs(100)," *Phys. Rev. Lett.* 75(13): 2542 (1995)
22. E. C. Le Ru, A. J. Bennett, C. Roberts and R. Murray, "Strain and electronic interactions in InAs/GaAs quantum dot multilayers for 1300 nm emission," *J. Appl. Phys.* 91(3): 1365 (2002).

23. K. Sears, H. Tan, M. Buda, J. Wong-Leung and C. Jagadish, "Growth and characterisation of InAs/GaAs quantum dots and diode lasers", *Proceedings of the 2006 International Conference on Nanoscience and Nanotechnology (ICONN)*, Brisbane, Australia, in press (2006).
24. P. M. Snowton, E. Herrmann, Y. Ning, H. D. Summers, P. Blood and M. Hopkinson, "Optical mode loss and gain of multiple-layer quantum-dot lasers," *Appl. Phys. Lett.* 78(18): 2629 (2001).
25. V. M. Ustinov, A. E. Zhukov, A. Yu. Egorov and N. A. Maleev, *Quantum Dot Lasers*, Oxford Science Publications, Oxford, UK, first edition, 2003.
26. K. Sears, M. Buda, H. H. Tan and C. Jagadish, "Modeling and characterization of InAs/GaAs quantum dot lasers grown by metal organic chemical vapor deposition," *J. Appl. Phys.*, submitted
27. S. Mokkalapati, H. H. Tan, C. Jagadish, "Integration of an InGaAs quantum dot laser with a low-loss passive waveguide using selective-area epitaxy", *IEEE Photonic Tech. Lett.*, 18(15), 1648 (2006).